Design of Longitudinal Controller for Automated Driving Bus

Takayuki Ando [1], Yongkang Zhou [2], Fujio Momiyama [2], Keiji Aoki [2], Bo Yang [1] & Kimihiko Nakano [1]
The University of Tokyo [1]
(4-6-1 Komaba, Meguro, Tokyo, 153-8508, Japan, t-ando@iis.u-tokyo.ac.jp)
Advanced Smart Mobility Co., Ltd. [2]
(4-6-1 Komaba, Meguro, Tokyo, 153-8508, Japan)

Abstract This paper describes the design of a longitudinal controller for an automated driving bus, which is expected to be a transportation method of the future. A linear longitudinal model is presented by approximating an aerodynamic drag force and rolling resistance force in a low speed range. Then, the feedback gains of a proportional integral (PI) controller for considering the longitudinal grade of the road are determined using a root locus method, with a constraint derived from the Chien–Hrones–Reswick method. A traffic light is predicted by the vehicle, so as to pass a signalized intersection smoothly. Further, a novel adaptive cruise control method is proposed for the automated driving bus, to reduce the acceleration of the vehicle. The performance of the controller is validated through pilot tests on public roads.

Keywords *Vehicle, Automated driving, Longitudinal control, Adaptive cruise control*

1 Introduction

In an aging society, the number of people who cannot drive increases, whereas the number of bus drivers decreases, owing to labor shortages. Thus, an automated driving bus is considered to be one solution for sustaining mobility. The "Intelligent Multimode Transit System" (IMTS) was demonstrated at the 2005 World Exposition in Aichi, Japan, using magnetic markers [1]. It traveled successfully on exclusive tracks with a barrier, at an average speed of 20 km/h and a maximum speed of 30 km/h. An automated driving bus in revenue service, developed in Oregon, USA, provided both lane keeping and S-curve precision docking in a mixed-traffic lane, while an operator controlled the speed [2]. Accidents caused by bus drivers are another problem that should be solved [3], [4], and the automated driving bus is expected to reduce such accidents.

This paper presents the design of a longitudinal controller for an automated driving bus, and the results of pilot tests on public roads using the proposed control. As shown in Table 1, there are several patterns where throttle or brake control is needed for the automated driving bus. For a public transportation bus, there is a high demand for reducing the magnitude of acceleration and deceleration, to prevent in-vehicle accidents. Thus, the maximum value of the acceleration and deceleration was set to be 2.0 m/s^2 during the pilot test. As the maximum speed of a typical public transportation bus is not high, it was set to be approximately 40 km/h and/or 35 km/h throughout the pilot studies, depending on location.

The longitudinal controller is designed using a root locus method of two feedback gains with a constraint, and its performance is validated through the pilot tests on public roads. This is valuable, as there have been few references validating a longitudinal controller for an automated driving bus on a public road.

Table 1. Throttle or brake control patterns

Throttle or brake control patterns	Situation
Follows speed defined through routes	Always
Adapts to road grade	At slopes
Changes speed according to traffic lights	At intersections
Conducts adaptive cruise control	Close to preceding vehicle

2 Design of longitudinal controller

To follow a reference speed defined through routes and to reduce acceleration of the vehicle, the speed and acceleration are treated as controlled values. The vehicle used for this study and the design method of the longitudinal controller are presented in the following sections.

2.1 Automated driving bus

Figure 1 shows the bus used for the pilot tests. It is accelerated by driving force generated from a diesel engine, and decelerated by braking force generated from an engine brake, exhaust retarder, or air-over hydraulic brake system. The throttle of the engine is controlled through an electrical signal, and the air pressure of the air-over hydraulic brake system is controlled through a control valve and a linear solenoid that simulates the position of pedals.

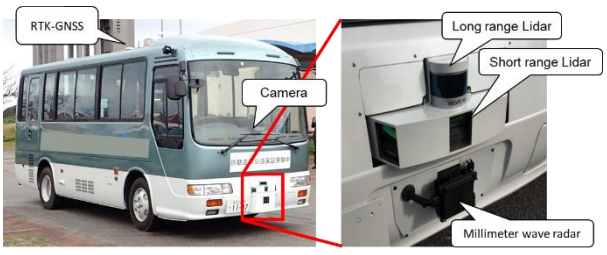

Figure 1. Sensors of automated driving bus

In addition, cameras, light detection and ranging (LiDAR) sensors, and millimeter-wave radars are equipped to detect preceding vehicles or other objects. A real-time kinematic global navigation satellite system (RTK-GNSS) is used to measure the position and speed of the vehicle.

2.2 Feedback controller

The longitudinal equation of motion of the vehicle is described as

$$m\ddot{x} = F_u - F_{aero} - F_{roll} - F_{grad}. \quad (1)$$

Here, m is the vehicle mass, $\ddot{x}$ is the vehicle longitudinal acceleration, F_u is the driving or braking force, F_{aero} is the aerodynamic drag force, F_{roll} is the rolling resistance force, and F_{grad} is the grade force [5]. Though the total mass of the vehicle changes with the number of passengers, it is assumed constant since the number of passengers is limited for the safety in pilot tests.

Assuming that F_u is modeled as an output of a first-order lag with dead time system of input u_a or u_b [6] [7], it is described as follows:

$$F_u = \begin{cases} \dfrac{K_a}{T_a s + 1} \cdot e^{-L_a s} \cdot u_a & (Throttle\ control) \\ \dfrac{K_b}{T_b s + 1} \cdot e^{-L_b s} \cdot u_b & (Brake\ control) \end{cases}. \quad (2)$$

In Equation (2), though some parameters are variable according to the condition of diesel engine or brake system, on the assumption that vehicle speed and acceleration is low, they are considered to be constant.

The aerodynamic drag force is generally described using vehicle longitudinal speed $V(:= \dot{x})$, as

$$F_{aero} = \frac{1}{2}\rho A_v C_d V^2, \quad (3)$$

where ρ is the air density, A_v is the frontal area of the vehicle, and C_d is the aerodynamic drag coefficient.

The rolling resistance force is generally described using vehicle longitudinal speed V as

$$F_{roll} = C_{roll} mg(c_0 + c_1 V + c_2 V^2), \quad (4)$$

where C_{roll} is a rolling resistance coefficient, and g is the gravitational acceleration.

The grade force is represented as a function of road grade angle θ_{grad} as

$$F_{grad} = mg \sin\theta_{grad}. \quad (5)$$

As both the aerodynamic drag force and rolling resistance force are resistance forces, the total resistance force F_{res} is defined as

$$F_{res} = F_{aero} + F_{roll}. \quad (6)$$

Figure 2 shows the relation between the travel resistance force F_{res} and vehicle longitudinal speed V. As long as V is under 11 m/s, F_{res} is approximated as a linear equation, and described as

$$F_{res} = a_0 + a_1 V = 403.2 + 60.7V. \quad (7)$$

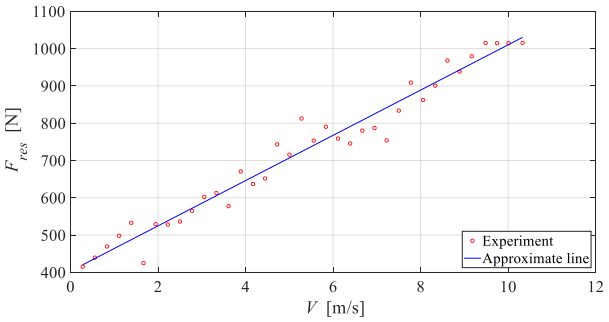

Figure 2. Identification of F_{res}

Adopting a proportional integral (PI) controller to follow the reference longitudinal speed V_r, as shown in Figure 3, the transfer function of this acceleration system is described as shown in Equation (8):

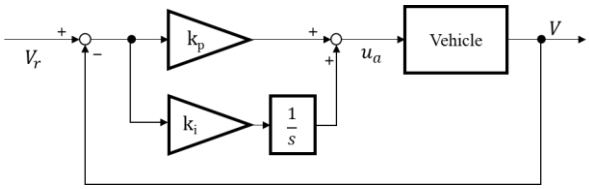

Figure 3. Feedback controller

$$V = \frac{K_a(k_p s + k_i)}{mT_a s^3 + (m + a_1 T_a)s^2 + (a_1 + K_a k_p)s + K_a k_i} \cdot V_r - \frac{s(T_a s + 1)(a_0 + mg\sin\theta_{grad})}{mT_a s^3 + (m + a_1 T_a)s^2 + (a_1 + K_a k_p)s + K_a k_i}. \quad (8)$$

In Equation (8), k_p is the proportional gain, and k_i is the integral gain. In addition, the dead time of the longitudinal equation of motion is ignored to derive Equation (8), since the effect of the dead time is small and difficult to be identified.

The integral gain k_i is described as follows, using the integral time T_i:

$$k_i = \frac{k_p}{T_i}. \quad (9)$$

Ziegler and Nichols (ZN) proposed a method of deciding parameters of a proportional-integral-differential (PID) controller, namely, proportional, integral, and differential gains [8]. In this method, the proportional gain is decided as the value by which the system begins to oscillate. It is necessary to conduct a

certain amount of experiments to obtain the proportional gain. They also proposed a way of determining integral time T_i using dead time L by Equation (10):

$$T_i = \frac{L}{0.3}. \tag{10}$$

Subsequently, Chien, Hrones, and Reswick (CHR) proposed that T_i is described as in Equation (11) when the system is approximated as a first-order lag system, where a time constant is expressed as T [9]:

$$T_i = 1.2T. \tag{11}$$

Though the ZN method and CHR method are both useful for determining the value of integral time T_i, at this time, Equation (11) is used to determine it, as the variation of identification of the time constant T is smaller than that of the dead time L. Through the experiment, T is identified as 3.3 s, as can be seen in Figure 4. Then, the relation between k_p and k_i is determined as shown in Equation (12), by substituting (11) into (9).

$$k_p = 4.0k_i. \tag{12}$$

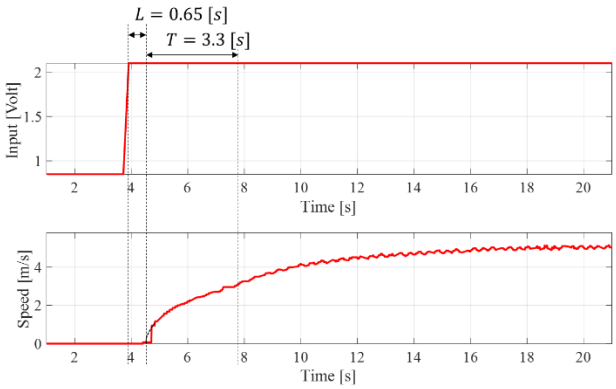

Figure 4. Identification of T

The root locus method is useful for determining the value of k_p and k_i. Figure 5 depicts 12 curve lines of the root locus for the main pole, which are represented by the "Original locus", and each line is a set of poles calculated with variable k_p and constant k_i. Considering the constraint expressed by Equation (12), a point with the constraint in each line is obtained, and these points are represented by "With constraint". Table 2 shows the values of the vehicle parameters used for calculation.

Table 2. Vehicle parameters

Vehicle parameters	Value
m	5200 kg
T_a	0.90 s
K_a	14280
a_1	60.7

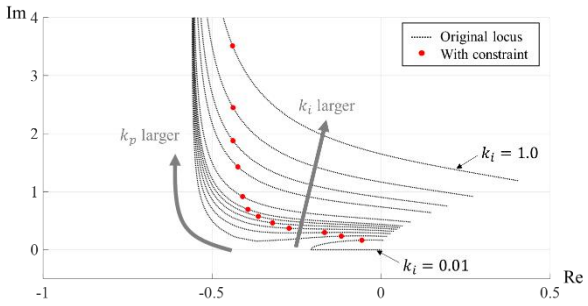

Figure 5. Root locus of main pole

Among these points, an optimal point is defined as the point where the damping ratio ζ is the highest. Figure 6 describes the results of a more detailed calculation near the optimal point. As shown in Figure 6, a point of $k_p = 0.188$ with $k_i = 0.047$ is found to be the optimal point. The maximum damping ratio is obtained as $\zeta_{max} = 0.572$. The optimal feedback gains for brake control are also determined by the same way as throttle control. In this paper, the effect of the longitudinal controller to the lateral dynamics is ignored, however, it will be necessary to be considered in some special cases.

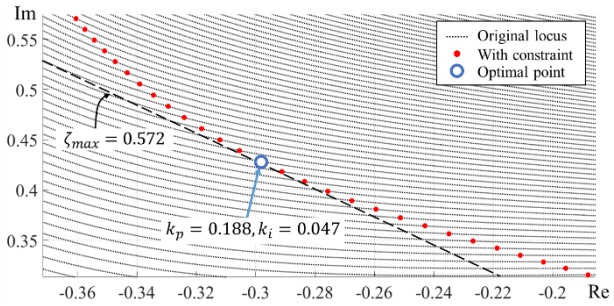

Figure 6. Optimal point of root locus for speed controller

To validate the method mentioned above, three sets of feedback gains (patterns I, II, and III) are examined, as depicted in Figure 7. The feedback gains of pattern I are the set of high gains. The feedback gains of pattern II are the set of low gains, with an extremely low damping ratio. The feedback gains of pattern III are set as representative of the optimal point. Bode diagrams for patterns I, II, and III are shown in Figures 8, 9, and 10, respectively. Here, the second term of the right hand side of Equation (8) is assumed zero. In Figure 8 (pattern I) the maximum magnitude is over 10 dB, and the corresponding frequency is relatively high because of the large feedback gains. In pattern II (Figure 9), the maximum magnitude is over 20 dB, and the corresponding frequency is relatively low because of the small feedback gains. In pattern III (Figure 10), which is near the optimal point, the maximum magnitude is approximately 3 dB.

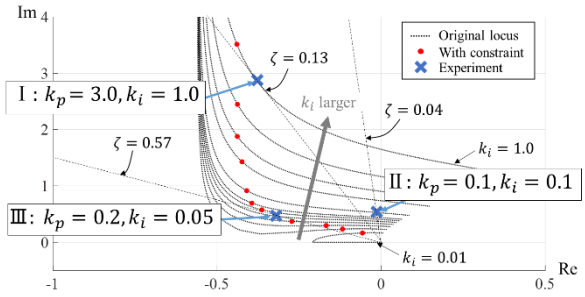

Figure 7. Optimal point of root locus for speed controller

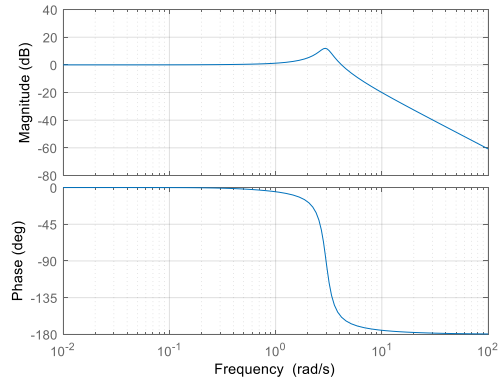

Figure 8. Bode diagram for pattern I

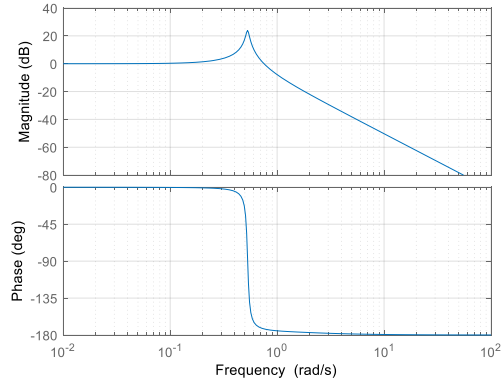

Figure 9. Bode diagram for pattern II

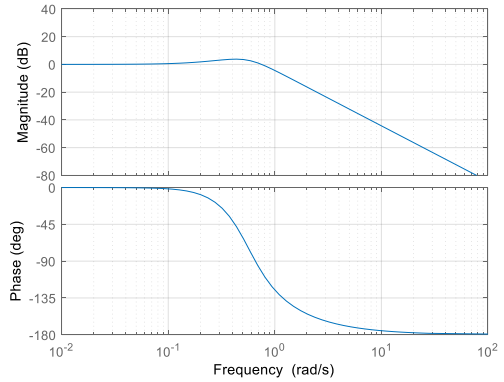

Figure 10. Bode diagram for pattern III

Vehicle experimental results for patterns I, II, and III, are shown in Figures 11, 12, and 13, respectively. In pattern I, a 50% overshoot and oscillations with high frequency to the step input of the reference speed are found. The feedback gains of pattern II produce over 100% overshoot in the same situation, whereas the overshoot of pattern III is very small (under 5%). These experimental results show that the longitudinal model simulates the motion of the actual vehicle well, and that the feedback gains of pattern III are the most suitable for the longitudinal control.

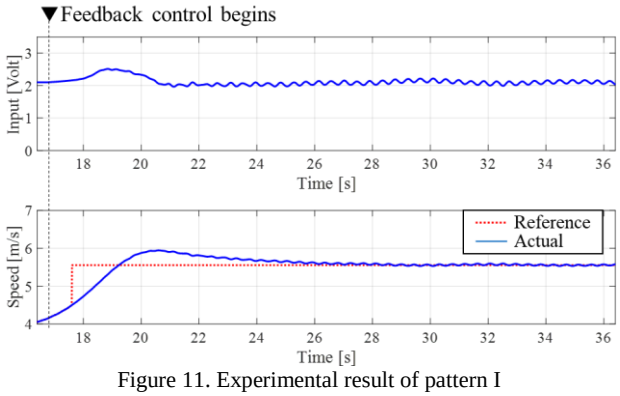

Figure 11. Experimental result of pattern I

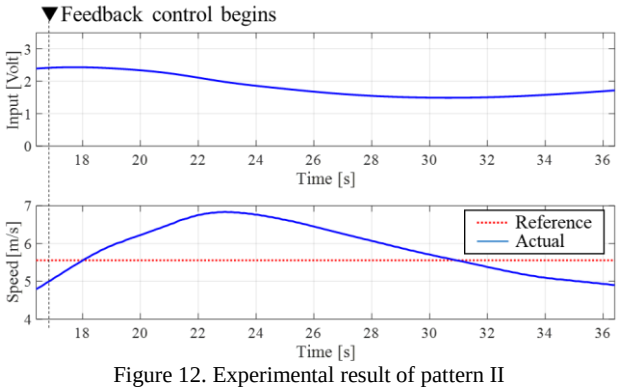

Figure 12. Experimental result of pattern II

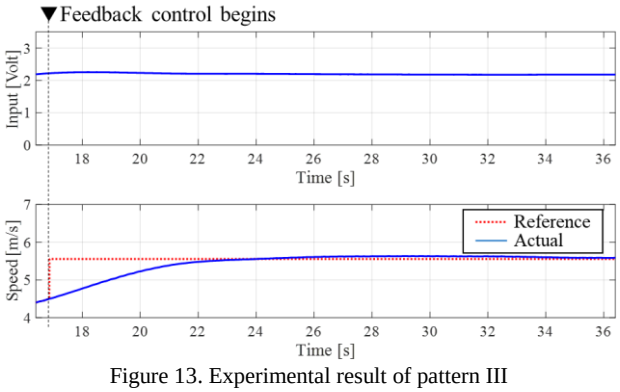

Figure 13. Experimental result of pattern III

2.3 Grade adaptation

A vehicle traveling at a slope is accelerated or decelerated by the gravity force caused by a road grade [10], as shown in Figure 14. The automated driving bus needs to consider the road grade in controlling the throttle valve and brake air pressure. The vehicle estimates the road grade under a center of gravity calculated from Equation (13), using the longitudinal acceleration a_{lon} and longitudinal speed V:

$$a_{grad} = g \sin \theta_{grad} = a_{lon} - \frac{dV}{dt}. \qquad (13)$$

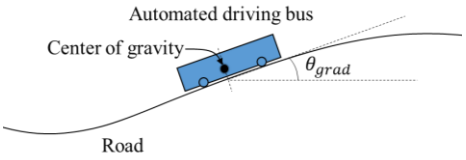

Figure 14. Road grade

2.4 Traffic light prediction control

The vehicle predicts a signal when it arrives at a signalized intersection. As shown in Figure 15, if a predicted traffic light turns to yellow or red before the vehicle passes the passage decision line, it decelerates and stops at in front of a stop line, or maintains a suitable gap from the preceding vehicle. A reference speed is always calculated considering the delay of the system to advance the deceleration of the vehicle in intersections according to a predicted light, as shown in Figure 16. To predict a light, the vehicle requires information of the cycles of the traffic lights in advance, such as the times the traffic light changes, and the difference between the local time of a traffic light and that of GNSS. Figure 17 shows a flow of traffic light prediction control.

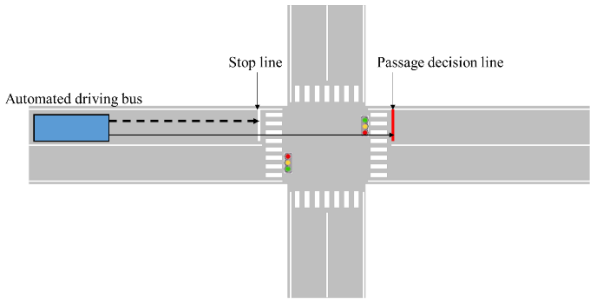

Figure 15. Stop line and passage decision line

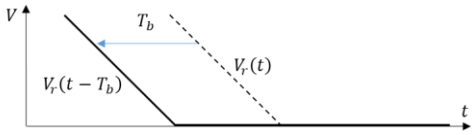

Figure 16. Stop line and passage decision line

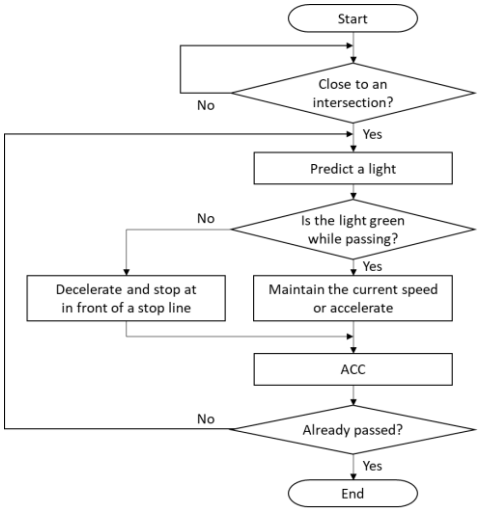

Figure 17. Flow of traffic light prediction control

2.5 Adaptive cruise control

Adaptive cruise control (ACC) has been studied and practically used in passenger vehicles and heavy vehicles [11] [12] [13]. Equation (14) is generally used to calculate the input of actuator u:

$$u = K_1 \left(L_f - \left(V_f \cdot T_0 + L_0\right)\right) + K_2\left(V_f - V\right). \qquad (14)$$

In Equation (14), L_f is the distance between a controlled vehicle and a preceding vehicle, V_f is the longitudinal speed of a preceding vehicle, T_0 is the time headway between the ego vehicle and the preceding vehicle, L_0 is a margin of distance between two vehicles, and K_1 and K_2 are control gains.

However, it is difficult to control the value of acceleration using Equation (14). In particular, for an automated driving bus, it is necessary to lower the acceleration to prevent in-vehicle accidents. As shown in Figure 18, the reference acceleration of the vehicle a_r is calculated using Equation (15), which aims to lower the acceleration and keep it constant. The reference acceleration a_r is the input of the longitudinal controller, and it is possible to use same controller mentioned in Section 2.2. The reference speed V_r is calculated by integrating the reference acceleration a_r.

$$a_r = \frac{0^2 - \left(V_f - V\right)^2}{2\left(L_f - V_f \cdot T_0 - L_0\right)} \qquad (15)$$

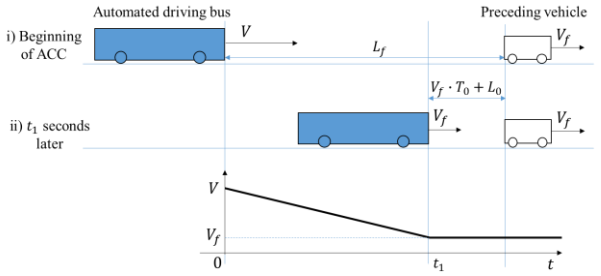

Figure 18. Adaptive cruise control (ACC) proposed for the bus

The two different types of ACC controllers mentioned above are compared through simulations, as shown in Figures 19 and 20. The parameters used in the simulation are shown in Table 3. After the absolute value of the acceleration of the vehicle using conventional ACC reaches over 1.93 m/s^2 when the vehicle detects a preceding vehicle 50 m ahead, its value gradually decreases to zero. To the contrary, the absolute value of acceleration of the vehicle using the novel ACC remains at approximately 1.19 m/s^2.

Table 3. Simulation parameters

Simulation parameters	Value
Initial V	11.1 m/s
Initial V_f	1.39 m/s
Initial L_f	50 m
T_0	1.5 s
L_0	5 m
K_1	0.04
K_2	0.4

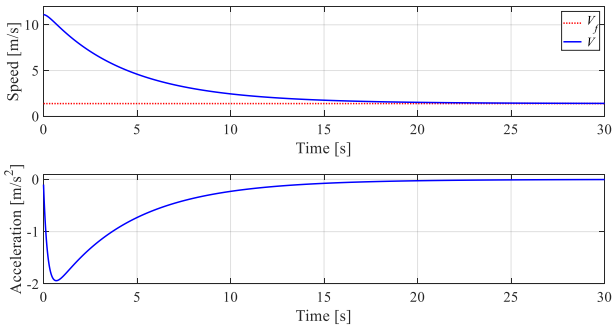

Figure 19. Simulation result of conventional ACC

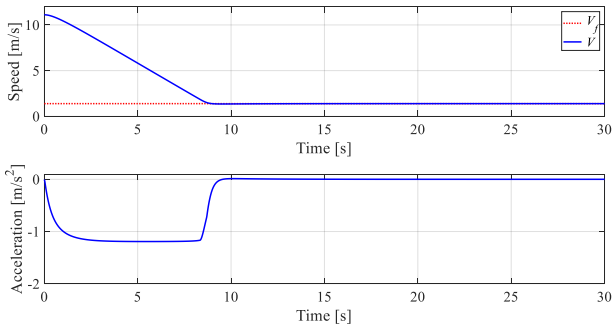

Figure 20. Simulation result of ACC for automated driving bus

For a platoon of vehicles, string stability is also important [11] [14]. If the transfer function from the range error of a vehicle to that of its following vehicle has a magnitude less than or equal to 1, it is string stability. Figure 21 shows the bode diagram of the transfer function obtained by numerical simulation using the novel ACC algorithm. It indicates that string stability is guaranteed since the magnitude of the transfer function is less than or equal to 0 dB.

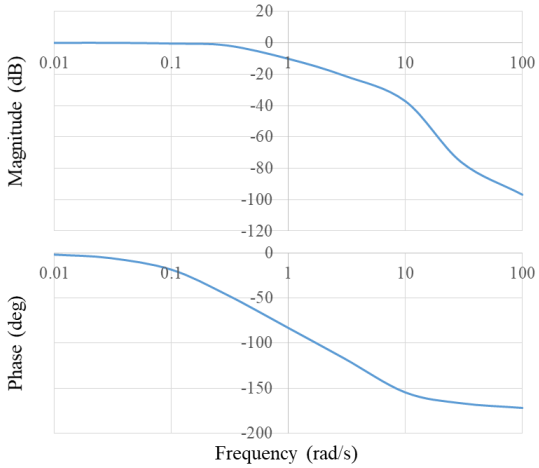

Figure 21. Bode diagram of the transfer function from the range error of a vehicle to that of its following vehicle

2.6 Total longitudinal controller

Considering all of the controllers mentioned above, a total longitudinal controller is constructed, as shown in Figure 22. To improve the response of the longitudinal speed, a feedforward controller is introduced. The relation between acceleration, speed and throttle was obtained by an experiment as shown in Figure 23. The output of the feedforward controller u_{ff} is calculated using the relation expressed by a two-dimensional array of a_r and V_r as written in Equation (16). The image of this array is also shown in Figure 22.

$$u_{ff} = F(a_r, V_r) \tag{16}$$

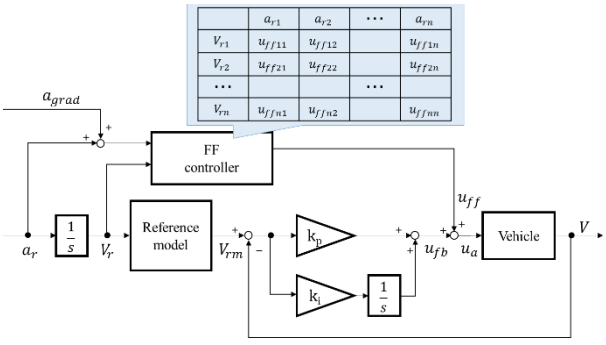

Figure 22. Total longitudinal controller

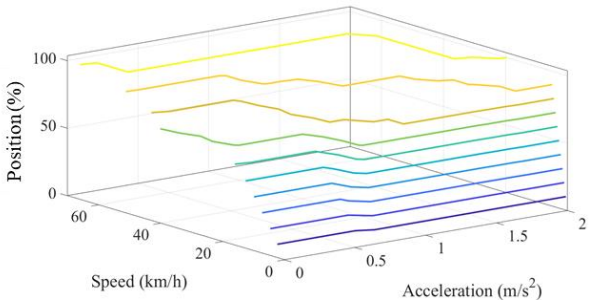

Figure 23. Relation between acceleration, speed and throttle

In addition, the reference model for the feedback controller is introduced as a first-order lag system of V_r, which is aimed to prevent the feedback controller from moving excessively. The acceleration generated from road grade a_{grad} is added to a_r, and becomes the input of the feedforward controller.

3 Experimental results of pilot test

Pilot tests of an automated driving bus with the longitudinal controller mentioned above were conducted in different traffic environments in Japan, as shown in Table 4. In an urban area, as the road grade is relatively small and most of the lane is not narrow, the maximum speed is set to 40 km/h. The test in this area aims to examine controllability, quick-deliverability, and social acceptance for young and elderly people living in that area. To the contrary, in rural areas, where the road grade is large and the lane is narrow, the maximum speed is set to 35 km/h. The aim of the test is to examine controllability, convenience, and social acceptance, mainly for elderly people living in that area.

Table 4. Pilot tests on public road

	Urban area	Rural area
Prefectures	Okinawa, Fukuoka	Hokkaido, Nagano, Shiga
Traffic density	Relatively high	Relatively low
Maximum grade	5 %	8 %
Maximum speed	40 km/h	35 km/h
Total Distance	450 km	330 km
Total Passengers	180	660

3.1 Base of throttle and brake controller

Figure 24 shows that the automated driving bus accelerates smoothly, and that the actual longitudinal speed of the vehicle follows the reference well. The delay of the actual speed from the reference speed is under 1.5 s, and the acceleration of the vehicle is under 0.5 m/s^2.

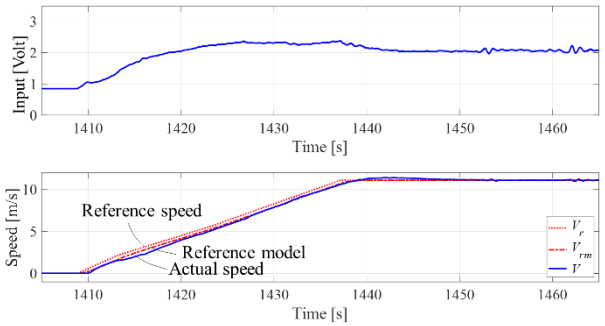

Figure 24. Experimental results of throttle control

Figure 25 shows that the vehicle decelerates smoothly, and that the actual longitudinal speed of it follows the reference well. The delay of the actual speed from reference speed is under 2.0 s, and the absolute value of acceleration of the vehicle is under 0.5 m/s^2.

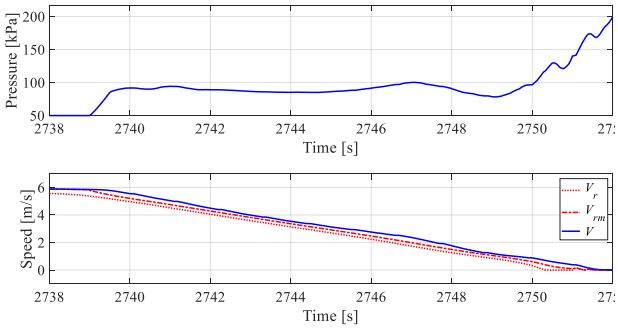

Figure 25. Experimental results of brake control

3.2 Grade adaptation

At the slope, the vehicle measures the road grade precisely and adapts to it with throttle or brake control, as shown in Figure 26. The actual speed follows the reference speed as well, as in the case where road is flat.

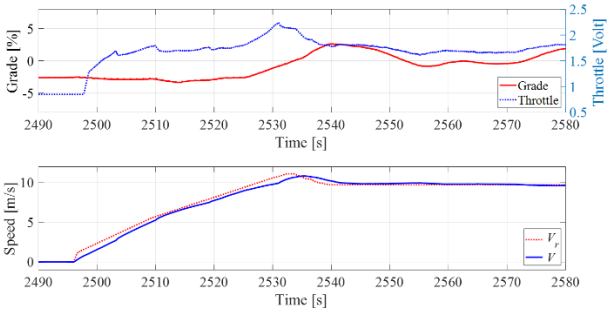

Figure 26. Experimental results of grade adaptation

3.3 Traffic light prediction control

At a signalized intersection, the vehicle predicts the traffic light at the time when it arrives, and decides as to whether it accelerates, decelerates, or keeps its speed. In Figure 27, because the predicted light is red, the vehicle

decelerates and stops in front of stop line. After the light changes to green, it starts.

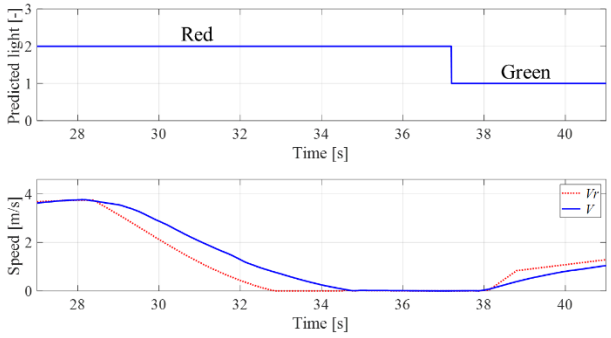

Figure 27. Experimental results of traffic light prediction control

3.4 Adaptive cruise control

Figure 28 shows a case in which the automated driving bus detects a preceding vehicle decelerating and stopping at an intersection. After the vehicle detects a preceding vehicle, it decelerates and stops at approximately 6 m behind the preceding vehicle, using the ACC algorithm proposed in Section 2.5. It is confirmed that the acceleration while decelerating is nearly constant, which is quite different from the conventional control [12]. The preceding vehicle waits for the traffic light to change when the vehicle longitudinal speed and relative speed are both zero. After the preceding vehicle starts, the automated driving bus follows it.

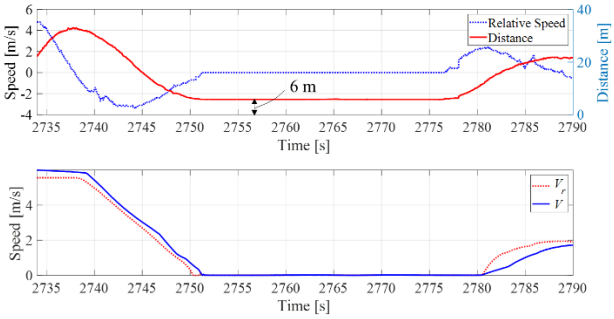

Figure 28. Experimental results of ACC

3.5 Total results

The total results of the pilot test are shown in Table 5. As for the urban area, the maximum overshooting rate is 5.6%, as designed in Section 2.2. The delay from reference reaches 2.3 s during decelerating at a downhill. The steady-state error is always small, as the longitudinal controller has integral control. Since the maximum acceleration is under 2.0 m/s^2, it can be concluded that the aim is achieved, as reducing jerk is demanded in improving the ride comfort. In contrast, in the rural area, all values are larger than in the urban area. The maximum overshooting rate and maximum delay from reference are especially large, as the road grade angle is large and with fluctuation.

Table 5. Experimental results

	Urban area	Rural area
Maximum overshooting rate	5.6%	7.6%
Maximum delay from reference	2.3 s	3.4 s
Maximum steady state error	2.2%	2.4%
Maximum acceleration	1.4 m/s^2	1.5 m/s^2
Maximum jerk	0.44 m/s^3	0.48 m/s^3

4 Conclusion

A method is proposed to design a longitudinal controller for an automated driving bus, with such buses expected to be a transportation method for elderly people who have difficulty in traveling. A simple linear longitudinal model is presented by approximating the aerodynamic drag force and rolling resistance force as linear in a low speed range. Then, the feedback gains of a PI controller are determined using the root locus method, with a constraint derived from the CHR method. The longitudinal controller also considers the road grade as measured by sensors. The vehicle predicts a traffic light by having the information of the traffic light in advance, so as to travel smoothly at signalized intersections. Finally, the novel ACC for the automated driving bus is proposed to select a desirable value of acceleration for the vehicle. The synthesis of those controllers is verified through pilot tests to be effective in achieving the goals of the pilot tests.

5 References

1. Keiji, A., Tomoyuki, D., Makoto, A. and Mitsuhisa, S., “Automated vehicle control technologies on Toyota IMTS”, Toyota Technical Review, Vol. 51, No .2, 2001, pp. 70-75
2. Huang, J., Tan, H. S., “Control System Design of an Automated Bus in Revenue Service”, IEEE Transactions on Intelligent Transportation Systems, Vol. 17, No. 10, 2016, pp. 2868 - 2878
3. Pontus, A. and Torbjorn, F., “Is there a pattern in European bus and coach incidents? A literature analysis with special focus on injury causation and injury mechanisms”, Accident Analysis and Prevention, 37, 2005, pp. 225-233
4. af Wahlberg, A. E., “Characteristics of low speed accidents with buses in public transport Part II”, Accident Analysis and Prevention, 36, 2004, pp. 63-71
5. Powell, B. K., Bailey, K. E., Cikanek, S. R., “Dynamic modeling and control of hybrid electric vehicle powertrain systems”, IEEE Control Systems Magazine, Vol. 18, No. 5, 1998, pp. 17-33
6. Bunker, B. J., Franchek, M. A., Thomason, B. E., “Robust multivariable control of an engine-dynamometer system”,

IEEE Transactions on Control Systems Technology, Vol. 5, No.2, 1997, pp. 189-199
7. Short, M., Pont, M. J., Huang, Q., "Simulation of vehicle longitudinal dynamics", Safety and Reliability of Distributed Embedded Systems, ESL04-01A-11, 2004, pp. 1-17
8. Ziegler, J. G. and Nichols, N. B. "Optimum setting for automatic controllers", Trans. ASME, Vol. 64, 1942, pp. 759-768
9. Hambali, N., Masngut, A., Ishak, A. A. and Janin, Z., "Process controllability for flow control system using Ziegler-Nichols (ZN), Cohen-Coon (CC) and Chien-Hrones-Reswick (CHR) tuning methods", IEEE International Conference on Smart Instrumentation, Measurement and Applications (ICSIMA), 2014, pp. 1-6
10. Bae, H. S., Ryu, J., Gerdes, J. C., "Road grade and vehicle parameter estimation for longitudinal control using GPS", Proceedings of the IEEE Conference on Intelligent Transportation Systems, 2001, pp 25-290
11. Liang, C., Peng, H., "Optimal adaptive cruise control with guaranteed string stability", Vehicle System Dynamics, 31, 1999, pp. 313-330.
12. Yanakiev, D., Kanellakopoulos, I., "Speed tracking and vehicle follower control design for heavy-duty vehicles", Vehicle System Dynamics, Vol. 25, No. 4, 1996, pp. 251-276
13. Li, S., Li, K., Rajamani, R. and Wang, J., "Model predictive multi-objective vehicular adaptive cruise control", IEEE Transactions on Control Systems Technology, Vol. 19, No. 3, 2011, pp. 556-566.
14. Ioannou, P. A., and Chien, C. C., "Autonomous intelligent cruise control", IEEE Transactions on Vehicular technology, Vol. 42, No. 4, 1993, pp. 657-672.

Takayuki Ando received Master's degree in mechanical engineering from the University of Tokyo, Tokyo, Japan. He is currently working toward Ph. D. degree in mechanical engineering at the University of Tokyo. His Ph.D. research is the design of a controller for an automated driving bus. While working toward the Ph.D. degree, he has been working at Advanced Smart Mobility Co., Ltd.

Yongkang Zhou received Master's degree in electrical engineering from Waseda University, Fukuoka, Japan. His research at Waseda University IPS Research Center concerned stability of autonomous driving. He has been working at Advanced Smart Mobility Co., Ltd.

Fujio Momiyama received Ph.D. degree in mechanical engineering from Nihon University, Tokyo, Japan. He worked for Hino Motors, Horikiri Inc., and Nihon University, and has been working for Advanced Smart Mobility Co., Ltd. His research concerns the longitudinal/lateral motion and ride quality modeling and the design principle for buses and trucks.

Keiji Aoki received Bachelor's in science and engineering from Nihon University, Tokyo, Japan. He worked at Toyota Motor Corporation and was project leader of the IMTS demonstrated at the 2005 World Exposition. He has been the founder and president of Advanced Smart Mobility Co., Ltd.

Bo Yang received Bachelor's degree in Mechanical Engineering from Huazhong University of Science and Technology, China, and was enrolled in the Ph.D. course of the University of Tokyo in 2014. Currently he is a project researcher at the Institute of Industrial Science, the University of Tokyo. His research interests include the development and evaluation of automated driving systems and advanced driver assistance systems.

Kimihiko Nakano obtained Master's and Ph.D. degrees in mechanical engineering from the University of Tokyo, Tokyo, in 1997 and 2000, respectively. After working for Yamaguchi University, he was assigned as Associate Professor of the University of Tokyo in 2006, and was promoted to Professor in 2018. His major research interests are in dynamics and control of vehicles, and human factors related to automobiles.